

Kinetic and potential parts of nuclear symmetry energy: the role of Fock terms

Qian Zhao^{1,2}, Bao Yuan Sun^{1,2} and Wen Hui Long^{1,2}

¹ School of Nuclear Science and Technology, Lanzhou University, Lanzhou 730000, People's Republic of China

² Key Laboratory of Special Function Materials and Structure Design, Ministry of Education, Lanzhou 730000, People's Republic of China

E-mail: sunby@lzu.edu.cn

Received 9 February 2015, revised 14 May 2015

Accepted for publication 5 June 2015

Published 20 July 2015



CrossMark

Abstract

The density dependence of nuclear symmetry energy is studied within the covariant density functional (CDF) theory in terms of the kinetic energy, isospin-singlet, and isospin-triplet potential energy parts of the energy density functional. When the Fock diagram is introduced, it is found that both isospin-singlet and isospin-triplet components of the potential energy play an important role in determining the symmetry energy. At high densities, a strong density-dependent behavior is revealed in the isospin-triplet potential part of the symmetry energy. In addition, the inclusion of the Fock terms in the CDF theory reduces the kinetic part of the symmetry energy and may lead to negative values at the supranuclear density region, which is regarded partly as the effect of the nuclear tensor-force components. The results demonstrate the importance of the Fock diagram in the CDF theory on the isospin properties of the in-medium nuclear force at high densities, especially from the isoscalar-meson coupling channels.

Keywords: symmetry energy, nuclear matter, covariant density functional theory, relativistic Hartree–Fock theory

(Some figures may appear in colour only in the online journal)

1. Introduction

The nuclear symmetry energy E_S , as defined by the difference of the binding energy per nucleon E_b in symmetric nuclear matter (SNM) and in pure neutron matter (PNM), plays an essential role in understanding the isospin-dependent aspects in nuclear physics and the

critical issues in astrophysics, such as neutron skin thickness and dipole excitation modes of stable or exotic nuclei, as well as the radius and cooling mechanism of neutron stars [1–8].

Various nuclear models have been applied to the exploration of the symmetry energy. Among the phenomenological approaches, two typical nuclear energy density functional (EDF) theories, the non-relativistic Skyrme–Hartree–Fock (SHF) [9] and relativistic mean field (RMF) [10–13] theories, are widely used for studying the issues related to symmetry energy. Recently, the density dependence of the symmetry energy E_S has been analyzed systematically in the SHF theory with 21 sets of Skyrme interactions [14] and in RMF theory with 23 sets of nonlinear, density-dependent, or point-coupling interactions [15]. It was found that important deviations of predicted E_S values appear beyond the nuclear saturation density ρ_0 . Besides, the density dependence of E_S can also be described by microscopic calculations, such as variational approaches [16], Brueckner–Hartree–Fock (BHF) approaches [17–19], and chiral effective field theory [20]. These calculations predict a relatively narrow band compared to the data extracted from the isobaric analog states experiments [21] below the saturation density, while the model deviations still remain at higher densities.

Until recently, extensive attention has been paid to the aspect of the theoretical model uncertainties in terms of the statistical error estimates of the models' parameters [22–29]. Since the EDF theories are effective approaches, and their parameters in effective interactions are often determined by fitting to empirical data such as masses of several selected double-magic nuclei and properties of nuclear matter at the saturation density ρ_0 , the theoretical error bars are unavoidably introduced when they are extrapolated to the density region beyond ρ_0 . Therefore, a stringent constraint on the equation of state at supranuclear densities from terrestrial experiments or astrophysical observations could be used to refine the EDF parametrization and reduce the uncertainties in predicting E_S at high densities.

With the inclusion of the Fock diagrams of the meson-nucleon couplings, the density-dependent relativistic Hartree–Fock (RHF) theory [30] has been developed, and it has achieved impressive success in describing the ground state [30–39] and excitation [40–42] properties of finite nuclei. Both RMF and RHF theories belong to the covariant density functional (CDF) theory. It has been found that the inclusion of the Fock terms strongly affects the density-dependent behaviors of the symmetry energy at high densities and, in turn, the radius and cooling process of neutron stars [3, 4, 43]. In particular, significant contributions to the symmetry energy have been found from the Fock terms of the isoscalar σ and ω couplings in contrast to the RMF, and the neutron-star properties determined by the density-dependent RHF theory were shown to be in fairly good agreement with the data.

In principle, the symmetry energy reflects the isospin-related properties of the in-medium nucleon–nucleon (NN) interactions, i.e., neutron–neutron (nn) and proton–proton (pp) interactions versus neutron–proton (np) interactions [44]. In view of the lack of enough knowledge about the isospin dependence of in-medium nuclear interactions, the investigation of the symmetry energy, especially its behavior at high densities, from a variety of theoretical models, together with the constraints from experiments such as heavy-ion collisions [7], could provide an efficient probe about the isospin nature of the nuclear force.

The isospin structure of the in-medium NN interaction can be analyzed by decomposing the two-body potentials into two-nucleon isospin-singlet ($T=0$) and isospin-triplet ($T=1$) states. In the microscopic BHF approach, $T=0$ and $T=1$ components can be obtained by the partial wave decomposition of the potential energy. Thus, the contributions from the different spin-isospin channels to E_S and the density slope parameter L can be analyzed quantitatively, and it is found that the spin-triplet and isospin-singlet channel give the major contributions, confirming the important role of the tensor force [45]. In the CDF theory, the isospin structure of the in-medium NN interaction is naturally taken into account via the meson exchange

mechanism. However, detailed analysis of the isospin decomposition of the potential energy into different contributions to the symmetry energy has not been carried out yet in the CDF framework. Particularly, in the density-dependent RHF theory, how the Fock diagram affects the isospin-related nature of the in-medium NN interactions need to be clarified.

In addition, the kinetic EDF ε_k has been identified as a particularly good indicator of the short-range correlations due to the tensor force in the nuclear ground state [45–50]. It is found that the contribution from ε_k to the symmetry energy is strongly reduced and even becomes negative due to such correlations when compared to the non-interacting case [46, 48–50]. In CDF theory, the kinetic EDF ε_k , which contains the self-energies, gets the in-medium NN interaction involved as well [3]. It is now possible in the RHF theory to extract the nuclear tensor interaction directly from the Fock diagrams of various meson-nucleon couplings [39], and distinct tensor effects are found in the exploration of the isospin properties of nuclear matter and neutron star structures [43]. Thus, it is interesting to study the in-medium effects hidden in ε_k within the CDF theory, in particular the contribution due to the short-range correlations. In this work, in terms of kinetic energy, the $T = 0$ and $T = 1$ potential energy parts of the EDF, we will study the isospin dependence of in-medium NN interactions based on several selected CDF energy functionals and their influence on the nuclear symmetry energy, especially the role of the Fock terms.

2. Theoretical framework

The detailed formalism of the CDF theory, in particular the RHF theory for nuclear systems, can be found in [3, 39, 51]. In this section we briefly recall the main CDF formalism and then present the decomposition of the EDF in terms of the two-nucleon isospin states. In the CDF theory, the EDF is obtained by taking the expectation value of the Hamiltonian with respect to the Hartree–Fock ground state. It consists of three parts

$$\varepsilon_k = \sum_{p s \tau} \bar{u}(p, s, \tau)(\boldsymbol{\gamma} \cdot \mathbf{p} + M)u(p, s, \tau), \quad (1)$$

$$\varepsilon_\phi^D = \frac{1}{2} \sum_{p_1 s_1 \tau_1} \sum_{p_2 s_2 \tau_2} \bar{u}(p_1, s_1, \tau_1) \bar{u}(p_2, s_2, \tau_2) \Gamma_\phi(1, 2) \frac{1}{m_\phi^2} u(p_2, s_2, \tau_2) u(p_1, s_1, \tau_1), \quad (2)$$

$$\varepsilon_\phi^E = -\frac{1}{2} \sum_{p_1 s_1 \tau_1} \sum_{p_2 s_2 \tau_2} \bar{u}(p_1, s_1, \tau_1) \bar{u}(p_2, s_2, \tau_2) \Gamma_\phi(1, 2) \frac{1}{m_\phi^2 + \mathbf{q}^2} u(p_1, s_1, \tau_1) u(p_2, s_2, \tau_2), \quad (3)$$

with $\phi = \sigma, \omega, \rho, \pi$. Here ε_k denotes the kinetic EDF, and ε_ϕ^D and ε_ϕ^E correspond to the Hartree (direct) and Fock (exchange) terms of the potential EDF, which come from the two-body interaction parts of the Hamiltonian [3, 39]. In the above expressions, the $\Gamma_\phi(1, 2)$ represent various meson- NN interaction vertices. The Dirac spinors $u(p, s, \tau)$ depend on the momentum p , spin s , and isospin τ

$$u(p, s, \tau) = \left[\frac{E^* + M^*}{2E^*} \right]^{1/2} \begin{pmatrix} 1 \\ \frac{\boldsymbol{\sigma} \cdot \mathbf{p}^*}{E^* + M^*} \end{pmatrix} \chi_s \chi_\tau, \quad (4)$$

where χ_s and χ_τ denote the spin and isospin wave functions, respectively. The starred quantities, which obey the relativistic mass-energy relation $E^{*2} = M^{*2} + \mathbf{p}^{*2}$, are defined as

$$M^* = M + \Sigma_S(p), \quad \mathbf{p}^* = \mathbf{p} + \hat{\mathbf{p}}\Sigma_V(p), \quad E^* = E - \Sigma_0(p), \quad (5)$$

where Σ_S is the scalar self-energy, and Σ_0 and Σ_V correspond to the time and space components of the vector self-energy, respectively. In the following we use the notation $\tau = 1/2$ for neutron (n), and $\tau = -1/2$ for proton (p). Then, we can define the two-nucleon isospin-singlet state $|00\rangle$ and isospin-triplet states $|11\rangle$, $|10\rangle$, $|1-1\rangle$ as

$$|00\rangle = \frac{1}{\sqrt{2}} \left\{ \chi_n(1)\chi_p(2) - \chi_p(1)\chi_n(2) \right\}, \quad (6)$$

$$|11\rangle = \chi_n(1)\chi_n(2), \quad (7)$$

$$|10\rangle = \frac{1}{\sqrt{2}} \left\{ \chi_n(1)\chi_p(2) + \chi_p(1)\chi_n(2) \right\}, \quad (8)$$

$$|1-1\rangle = \chi_p(1)\chi_p(2). \quad (9)$$

Thus, the Hartree (direct) potential EDF (see equation (2)) can be divided into the isospin-singlet ($T=0$) and isospin-triplet ($T=1$) parts

$$\varepsilon_\phi^D = \varepsilon_{\phi,T=0}^D + \varepsilon_{\phi,T=1}^D, \quad (10)$$

where

$$\varepsilon_{\phi,T=0}^D = \frac{1}{2} \sum_{p_1 s_1} \sum_{p_2 s_2} \bar{u}(p_1, s_1) \bar{u}(p_2, s_2) \langle 00 | \frac{\Gamma_\phi(1, 2)}{m_\phi^2} | 00 \rangle u(p_2, s_2) u(p_1, s_1), \quad (11)$$

$$\begin{aligned} \varepsilon_{\phi,T=1}^D = \frac{1}{2} \sum_{p_1 s_1} \sum_{p_2 s_2} \bar{u}(p_1, s_1) \bar{u}(p_2, s_2) & \left\{ \langle 11 | \frac{\Gamma_\phi(1, 2)}{m_\phi^2} | 11 \rangle + \langle 10 | \frac{\Gamma_\phi(1, 2)}{m_\phi^2} | 10 \rangle \right. \\ & \left. + \langle 1-1 | \frac{\Gamma_\phi(1, 2)}{m_\phi^2} | 1-1 \rangle \right\} u(p_2, s_2) u(p_1, s_1). \end{aligned} \quad (12)$$

Similarly, the corresponding parts of the Fock terms $\varepsilon_{\phi,T=0}^E$ and $\varepsilon_{\phi,T=1}^E$ can also be obtained. As a result, the binding energy per nucleon E_b in nuclear matter for a given baryonic density ρ_b and isospin asymmetry $\delta \equiv (\rho_n - \rho_p)/\rho_b$ can be decomposed as:

$$E_b(\rho_b, \delta) = E_{b,k} + E_{b,T=0}^D + E_{b,T=0}^E + E_{b,T=1}^D + E_{b,T=1}^E, \quad (13)$$

where $E_{b,k}$ is the kinetic part, $E_{b,T=0}^D$ and $E_{b,T=0}^E$ are the Hartree and Fock terms of the $T=0$ potential energy, and $E_{b,T=1}^D$ and $E_{b,T=1}^E$ are those of the $T=1$ potential energy.

In general, the binding energy per nucleon $E_b(\rho_b, \delta)$ of asymmetric nuclear matter can be expanded in a Taylor series with respect to the isospin asymmetry parameter δ , and the density-dependent symmetry energy is then deduced from the second-order coefficient as,

$$E_S(\rho_b) = \frac{1}{2} \frac{\partial^2 E_b(\rho_b, \delta)}{\partial \delta^2} \Bigg|_{\delta=0}. \quad (14)$$

To shed light on the density dependence of the symmetry energy, E_S can be further expanded around the nuclear saturation density ρ_0 as:

$$E_S(\rho_b) = J + L\xi + \mathcal{O}(\xi^2), \quad (15)$$

where $\xi \equiv (\rho_b - \rho_0)/3\rho_0$, $J \equiv E_S(\rho_0)$ corresponds to the symmetry energy at saturation density ρ_0 , and the density slope L is,

$$L = 3\rho_0 \left. \frac{\partial E_S}{\partial \rho_b} \right|_{\rho_b=\rho_0}. \quad (16)$$

With the expression in equation (13), the symmetry energy E_S and its density slope L can be divided into:

$$E_S(\rho_b) = E_{S,k} + E_{S,T=0}^D + E_{S,T=0}^E + E_{S,T=1}^D + E_{S,T=1}^E, \quad (17)$$

$$L = L_k + L_{T=0}^D + L_{T=0}^E + L_{T=1}^D + L_{T=1}^E. \quad (18)$$

Combining equations (1) and (4), the kinetic EDF can be expressed as:

$$\varepsilon_k = \frac{1}{\pi^2} \sum_{i=n,p} \int_0^{k_{F,i}} M \hat{M} p^2 dp + \frac{1}{\pi^2} \sum_{i=n,p} \int_0^{k_{F,i}} p \hat{P} p^2 dp \equiv \varepsilon_k^M + \varepsilon_k^P, \quad (19)$$

where $\hat{M} = M^*/E^*$, $\hat{P} = \mathbf{p}^*/E^*$, and ε_k^M and ε_k^P denote the contributions from the nucleon mass and momentum, respectively. Then, the contribution from ε_k to symmetry energy, namely, the kinetic part of E_S , can be decomposed as,

$$E_{S,k} = E_{S,k}^M + E_{S,k}^P. \quad (20)$$

In order to investigate the in-medium effects hidden in the $E_{S,k}$, we separate \hat{M} into:

$$\hat{M} = \frac{M}{E^*} + \frac{\Sigma_S^D}{E^*} + \sum_{\phi} \frac{\Sigma_S^{E,\phi}}{E^*}. \quad (21)$$

Correspondingly, $E_{S,k}^M$ can be decomposed according to the components of the self-energy.

3. Results and discussion

In this work, the calculations are carried out by utilizing the RHF functionals PKO1 [30] and PKA1 [31] and compared with results from the RMF ones TW99 [52] and PKDD [53]. They have been applied in studies of the bulk properties of asymmetric nuclear matter and neutron stars, and significant differences in the predicted symmetry energy have been revealed [3, 4]. For the RMF calculations with TW99 and PKDD, only the Hartree contributions are involved, whereas both Hartree and Fock terms contribute to the RHF results of PKO1 and PKA1. Due to the limitation of the approach itself, the π and ρ -tensor couplings are missing in TW99 and PKDD, while PKO1 contains the π couplings, and both are involved in PKA1.

3.1. Density dependence of symmetry energy

In figure 1, the decomposition of the binding energy per nucleon E_b into the kinetic energy part $E_{b,k}$ and isospin-singlet and isospin-triplet potential energy parts $E_{b,T=0}$ and $E_{b,T=1}$ are plotted for SNM ($\delta = 0$) and PNM ($\delta = 1$) with four selected CDF effective interactions. It is found that at high densities the contributions from the $T = 1$ potential parts are enhanced in PNM, whereas the terms $E_{b,k}$ are slightly weakened as compared with those in SNM. In addition, the $T = 0$ part $E_{b,T=0}$, which is attributed to the np interaction and dominated by the Hartree terms, shows a relatively small contribution in SNM and vanishes in PNM. When the baryonic density is smaller than about 0.2 fm^{-3} , it is seen that all the effective interactions

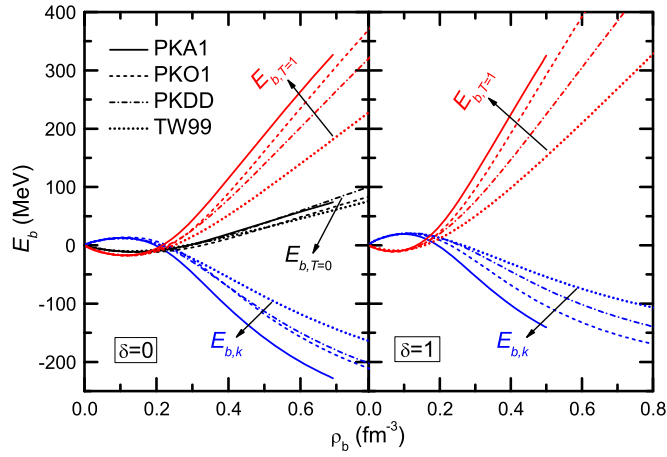


Figure 1. Decomposition of the binding energy per nucleon E_b in symmetric nuclear matter ($\delta = 0$, left panel) and pure neutron matter ($\delta = 1$, right panel), namely, the kinetic energy $E_{b,k}$, isospin-singlet potential energy $E_{b,T=0}$, and isospin-triplet potential energy $E_{b,T=1}$ as functions of baryonic density ρ_b . The results are calculated with the RHF models PKO1 and PKA1 and with the RMF models TW99 and PKDD.

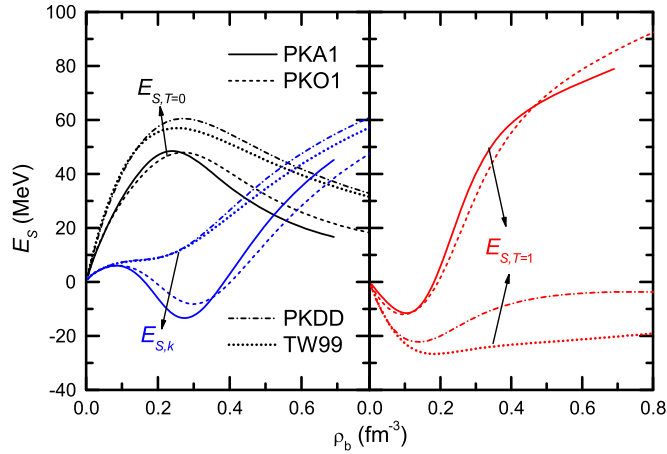


Figure 2. Decomposition of the nuclear symmetry energy E_S , namely, the kinetic energy part $E_{S,k}$, isospin-singlet potential part $E_{S,T=0}$ (left panel), and isospin-triplet potential part $E_{S,T=1}$ (right panel), as functions of baryonic density ρ_b . The results are calculated with the RHF models PKO1 and PKA1 in comparison with the RMF ones TW99 and PKDD.

predict nearly the same density-dependent behavior for the different components of E_b , while the deviations among the models become larger with increasing density. Therefore, it is expected that distinct model deviations on the density and isospin dependence of these components will lead to some uncertainty in the symmetry energy.

In terms of isospin decomposition, we then obtain three components of nuclear symmetry energy: the kinetic energy contribution $E_{S,k}$, the isospin-singlet potential contribution

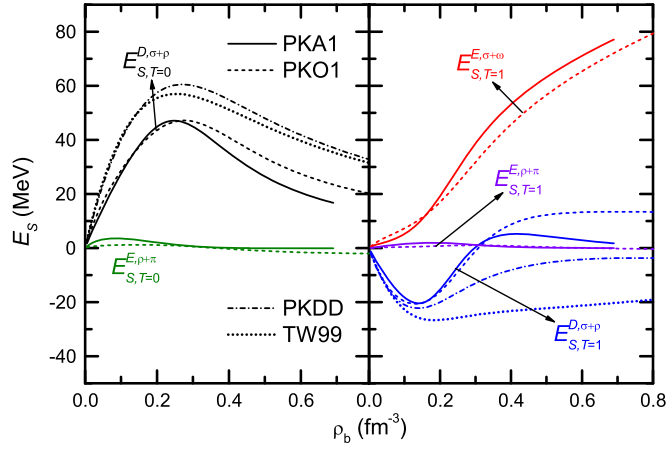


Figure 3. The isospin-singlet potential symmetry energy $E_{S,T=0}$ is decomposed into a Hartree part $E_{S,T=0}^{D,\sigma+\rho}$ from the σ - and ρ -meson coupling channels, and a Fock part $E_{S,T=0}^{E,\rho+\pi}$ from the ρ - and π -meson coupling channels, as functions of baryonic density ρ_b (left panel). The isospin-triplet potential symmetry energy $E_{S,T=1}$ is divided into a Hartree part $E_{S,T=1}^{D,\sigma+\rho}$ from the σ - and ρ -meson coupling channels, a Fock part $E_{S,T=1}^{E,\rho+\pi}$ from the ρ - and π -meson coupling channels, and a Fock part $E_{S,T=1}^{E,\sigma+\omega}$ from the σ - and ω -meson coupling channels (right panel). The results are calculated with the RHF effective interactions PKO1 and PKA1 and with the RMF ones TW99 and PKDD.

$E_{S,T=0} = E_{S,T=0}^D + E_{S,T=0}^E$, and the isospin-triplet potential contribution $E_{S,T=1} = E_{S,T=1}^D + E_{S,T=1}^E$, as shown in figure 2. One should notice that the contribution to E_S from the Hartree term in the ω -vector coupling channel is vanishing because of its isoscalar nature [3]. The symmetry energy deduced from the $T = 0$ and $T = 1$ components of the Hartree term in the ω -vector coupling channel actually compensate each other, i.e., $E_{S,T=0}^{D,\omega} + E_{S,T=1}^{D,\omega} = 0$. Hence, in the following discussion (also in figure 2) we do not include these parts.

From figure 2, it is seen that sizable deviations between the RMF and RHF results arise, even in the low-density region. For $E_{S,k}$ and $E_{S,T=0}$, the RMF models give larger values than the RHF ones, while the opposite trend occurs for $E_{S,T=1}$. Among the three components, $E_{S,T=1}$ displays the most distinct deviation between the RMF and RHF results, which leads to a stiffer symmetry energy in the RHF at higher densities, as already shown in [3]. In addition, it is seen in the RMF that the $E_{S,k}$ and $E_{S,T=0}$ terms dominate the density dependence of the symmetry energy at supranuclear densities, while all three components are non-negligible in the RHF cases. An analysis of in-medium NN interactions could be helpful to further clarify these results.

In figure 3 are shown the Hartree and Fock contributions to the isospin-singlet and isospin-triplet channels of the symmetry energy, namely, $E_{S,T=0}$ and $E_{S,T=1}$, for the selected CDF effective interactions. For the Hartree terms, namely, $E_{S,T=0}^{D,\sigma+\rho}$ (left panel) and $E_{S,T=1}^{D,\sigma+\rho}$ (right panel), the results are attributed to the σ - and ρ -meson coupling channels, and distinct deviations between the RMF and RHF are found in both the $T = 0$ and $T = 1$ channels. This could be explained by the difference in the meson-nucleon coupling constants of the selected effective interactions. It is interesting to see that when summing up the Hartree contribution of the $T = 0$ and $T = 1$ channels, namely, $E_{S,T=0}^{D,\sigma+\rho} + E_{S,T=1}^{D,\sigma+\rho}$, the model deviations on the total contribution from the Hartree term in effective NN interactions are reduced significantly. In

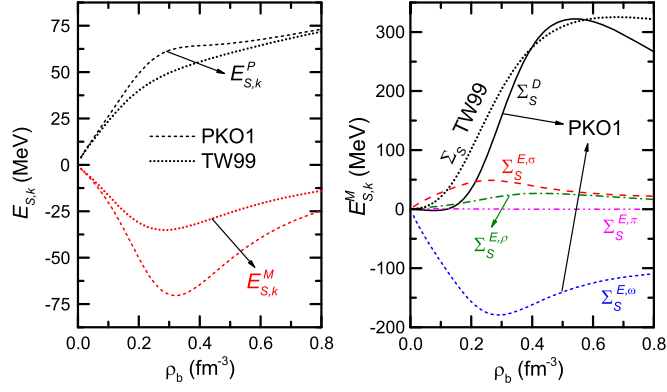


Figure 4. Decomposition of the kinetic part $E_{S,k}$ of the symmetry energy, namely, the mass-related and momentum-related terms $E_{S,k}^M$ and $E_{S,k}^P$, according to equation (20) (left panel). In the right panel, $E_{S,k}^M$ is separated again according to various components of the self-energy; see equation (21) for details. The results are calculated with the RHF effective interaction PKO1, in comparison with the RMF one TW99.

fact, the deviations on E_S between the RMF and RHF calculations come mainly from the Fock terms in effective NN interactions [3]. It can be clarified further by separating the contributions to the $T = 0$ and $T = 1$ symmetry energy from the Fock terms into the isoscalar and isovector meson-nucleon coupling channels, as shown in figure 3. We see that the contributions from the isovector meson fields, i.e., $E_{S,T=0}^{E,\rho+\pi}$ and $E_{S,T=1}^{E,\rho+\pi}$, are negligible due to the smaller isovector meson-nucleon coupling constants. However, the Fock contributions $E_{S,T=1}^{E,\sigma+\omega}$ of isoscalar mesons in the $T = 1$ channel exhibit rather stiff density-dependent behavior, which in turn leads to the distinct deviation on $E_{S,T=1}$ between the RMF and RHF calculations in figure 2. Notice that, via the Fock diagram, the isoscalar σ - and ω -meson account for only nn and pp interactions rather than the np interaction. It is therefore natural that the relevant contributions $E_{S,T=0}^{E,\sigma+\omega}$ vanish.

Now we turn to the discussion of the origin of the model deviations on the kinetic part $E_{S,k}$ of the symmetry energy from a viewpoint of meson-nucleon coupling channels. It is seen in figure 2 that the inclusion of the Fock terms in the RHF theory reduces remarkably the kinetic part $E_{S,k}$, as compared to the RMF results. At supranuclear densities of about $1 \sim 2.5 \rho_0$ the RHF results even become negative. To identify the physical mechanism, $E_{S,k}$ is further decomposed into the mass- and momentum-related terms via equation (20), i.e., $E_{S,k}^M$ and $E_{S,k}^P$, as plotted in the left panel of figure 4. It is seen that the deviations between the RMF and RHF results of $E_{S,k}$ are dominated by the mass-related part $E_{S,k}^M$ rather than the momentum-related one $E_{S,k}^P$, in which the self-energy Σ_V is negligible in the RHF results. To further clarify such model deviations, the right panel of figure 4 shows the contributions to $E_{S,k}^M$ from different terms of the scalar self-energy Σ_S , according to equation (21). It is found that the direct terms of the scalar self-energy Σ_S^D in both the RMF and RHF present similar contributions to $E_{S,k}^M$. For the Fock terms in PKO1, namely, $\Sigma_S^{E,\phi}$, a remarkably negative contribution to $E_{S,k}^M$ is found from the ω -meson coupling channel (denoted as $\Sigma_S^{E,\omega}$), while relatively weak but still considerable contributions come from the other coupling channels, eventually leading to a significant difference in the sign and magnitude of $E_{S,k}$ between the RMF and RHF results (see the left panel of figure 2). In fact, it has been demonstrated very

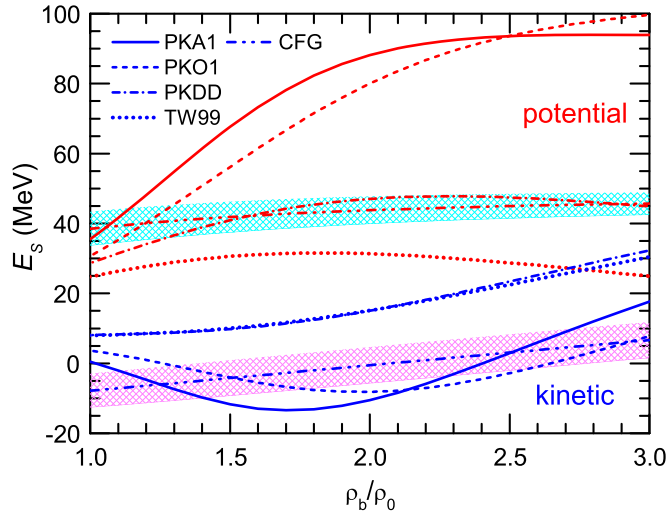


Figure 5. The density dependence of the kinetic (blue lines) and potential parts (red lines) of the symmetry energy, calculated with the RHF models PKO1 and PKA1 and with the RMF models TW99 and PKDD. For comparison, the referred lines (dash-dot-dotted) and regions with the error bar from the correlated Fermi gas (CFG) model [50] for the kinetic and potential parts are given as well.

recently that the nuclear tensor interactions are naturally enclosed in both the isoscalar and the isovector meson-nucleon coupling channels with the presence of the Fock diagrams in the RHF EDF [39, 43]. Consequently, the extra contributions from the Fock terms of the scalar self-energy to $E_{S,k}$ could be regarded partly as the effects of the nuclear tensor-force components therein, which is further related to the short-range correlation of the NN interactions, as already discussed in other models [45–49]. Actually, according to the expressions of the tensor-related EDF shown in [43], only the ω -meson via the Fock diagram could contribute the tensor-force component of the scalar self-energy.

To further clarify the effects of Fock terms on the density dependence of the symmetry energy, the calculated kinetic and potential parts of E_S at supranuclear densities with the CDF models are compared with the results with the correlated Fermi gas (CFG) model [50], as shown in figure 5. In the CFG model, the tensor force-induced short-range correlations between np pairs could shift nucleons to high momentum in SNM but have almost no effect in PNM. Thus, the kinetic part of the symmetry energy with tensor correlations at ρ_0 reduces to about -10 MeV in CFG, which differs significantly from $+12.5$ MeV for the widely used free Fermi gas model [50]. It is seen in figure 5 that the RHF model PKO1 and PKA1 could give more comparable values of $E_{S,k}$ with the CFG model at supranuclear densities, while the $E_{S,k}$ with the RMF is about $10 \sim 20$ MeV larger than CFG. Therefore, it is clear that the inclusion of the Fock terms in the CDF theory improve the description of the kinetic part of the symmetry energy. However, for the potential part of the symmetry energy, it is found that the RHF models give much larger values than the CFG model, which is attributed mainly to extra Fock contributions of isoscalar mesons in the RHF, as seen in figure 3. Hence, the experimental constraints on the potential part of E_S at supranuclear densities will pave the efficient way for improving the RHF EDF.

3.2. Symmetry energy properties at saturation density

It is also interesting to discuss the properties of the symmetry energy at nuclear saturation density. Table 1 shows the contributions from the kinetic energy (kin), isospin-singlet ($T=0$), and isospin-triplet ($T=1$) potential energy to the symmetry energy J and its density slope L for SNM at the saturation density ρ_0 , calculated with the selected CDFs. For comparison, we list also the results calculated using the microscopic BHF theory with the Argonne V18 potential plus the Urbana IX three-body force [45], where it is exhibited that J and L at ρ_0 are mainly dominated by the $T=0$ potential component and, hence, by the tensor component of the nuclear force. Among the CDF results, if one disregards the direct ω -vector coupling, the $T=0$ and $T=1$ components of the symmetry energy J determined by PKO1 and PKA1 are very close to the BHF results, while the RMF models (TW99 and PKDD) lead to a relatively large negative contribution in the $T=1$ channel. Such deviation between the RHF and RMF models, as seen in figure 3, is ascribed to extra contributions from the isoscalar coupling channels $E_{S,T=1}^{E,\sigma+\omega}$ via the Fock diagram. It has been argued that the dominance of the $T=0$ component in the symmetry energy at saturation density is due to the effect of the tensor component of the nuclear force through the 3S_1 $-{}^3D_1$ channel [45]. However, in the CDF calculations the Hartree potential energy term plays the role instead. For density slope parameter L , although the $T=0$ components in the CDF are similar to the BHF one, we see that dramatically large uncertainties occur in kinetic energy and the $T=1$ potential energy parts, where the RMF effective interaction TW99 shows the smallest deviations from the BHF ones. Thus, the density dependence of the symmetry energy at high densities becomes quite dissimilar, and the trend in the RHF cases is strongly enhanced.

To clarify the above discussion we extract further in table 2 the detailed contributions to the $T=0$ and $T=1$ potential symmetry energy from the different meson-nucleon coupling channels. It is observed that in the CDF the $T=0$ potential part of J mainly comes from the Hartree diagram, especially from the isoscalar σ -meson coupling channel, while the $T=1$ potential contribution to J results from the cancellation between the negative contribution of the Hartree term of the σ -meson and positive contributions of other terms. Due to the significant contribution to J from the Fock term of σ - and ω -mesons in the RHF models, the total $T=1$ potential symmetry energy at saturation density is very small for PKO1 and PKA1 effective interactions, close to the referred BHF calculations. Table 3 shows a similar decomposition of the density slope parameter L as table 2. It is found that the $T=0$ component of the density slope L mainly comes from the Hartree term in the σ -meson coupling channel, whereas for the $T=1$ component there exist very large uncertainties in sign and magnitude among the selected CDF calculations. It is seen that the inclusion of the Fock terms, particularly in the isoscalar channels (σ - and ω -couplings), leads to extra uncertainties on L and thus remarkable differences on the behavior of the symmetry energy at high densities.

3.3. Influence of theoretical model uncertainties

It should be noticed that the error estimates of theoretical models have been paid extensive attention in nuclear physics [22–29], and related works were collected as a focus issue recently [54]. It is revealed that the systematic model errors occur due to an imperfect modeling procedure: deficient parametrization, wrong assumptions, and missing physics due to our lack of knowledge. Since the parameters in effective EDF interactions are often determined by fitting to empirical data such as masses of several selected double-magic nuclei and properties of nuclear matter at ρ_0 , the theoretical error bars are unavoidably introduced

Table 1. Kinetic energy (kin), isospin-singlet ($T=0$), and isospin-triplet ($T=1$) potential energy contributions to the symmetry energy J and its density slope L at nuclear saturation density with the selected CDF effective interactions. The values (in MeV) in/out of the parentheses denote the results with/without the inclusion of the contribution from the Hartree term in the ω -meson coupling channel. The referred values are taken from the BHF calculations in [45].

	TW99	PKDD	PKO1	PKA1	Reference [45]
kin	8.0	8.1	3.7	0.5	-1.0
J $T=0$	51.0 (8.7)	50.8 (10.3)	38.8 (11.4)	42.4 (10.5)	44.2
$T=1$	-26.2 (16.1)	-22.1 (18.4)	-8.1 (19.3)	-5.7 (26.1)	-9.0
kin	5.9	5.0	-34.5	-69.6	14.9
L $T=0$	62.2 (-21.1)	78.2 (-9.7)	67.5 (0.8)	71.3 (-14.3)	69.1
$T=1$	-12.8 (70.5)	7.0 (94.9)	64.8 (131.4)	103.2 (188.7)	-17.5

Table 2. Contributions from different meson-nucleon coupling channels to the $T=0$ and $T=1$ potential symmetry energy at saturation density with the selected CDF effective interactions. Units are given in MeV.

J	Channel	TW99	PKDD	PKO1	PKA1
$T=0$	Γ_{σ}^D	47.6	46.2	36.2	38.4
	Γ_{ρ}^D	3.4	4.6	1.5	1.2
	$\Gamma_{\sigma+\omega}^E$	0.0	0.0	0.0	0.0
	$\Gamma_{\rho+\pi}^E$	0.0	0.0	1.2	2.8
$T=1$	Γ_{σ}^D	-36.4	-35.8	-24.6	-23.3
	Γ_{ρ}^D	10.1	13.7	4.4	3.5
	$\Gamma_{\sigma+\omega}^E$	0.0	0.0	11.5	12.2
	$\Gamma_{\rho+\pi}^E$	0.0	0.0	0.6	1.9

Table 3. Similar to table 2 but for density slope parameter L of symmetry energy.

L	Channel	TW99	PKDD	PKO1	PKA1
$T=0$	Γ_{σ}^D	62.5	69.5	63.8	79.4
	Γ_{ρ}^D	-0.3	8.7	3.7	-0.3
	$\Gamma_{\sigma+\omega}^E$	0.0	0.0	0.0	0.0
	$\Gamma_{\rho+\pi}^E$	0.0	0.0	-0.01	-7.9
$T=1$	Γ_{σ}^D	-11.9	-19.0	7.5	29.4
	Γ_{ρ}^D	-0.9	26.0	11.1	-0.9
	$\Gamma_{\sigma+\omega}^E$	0.0	0.0	44.3	73.4
	$\Gamma_{\rho+\pi}^E$	0.0	0.0	1.8	1.3

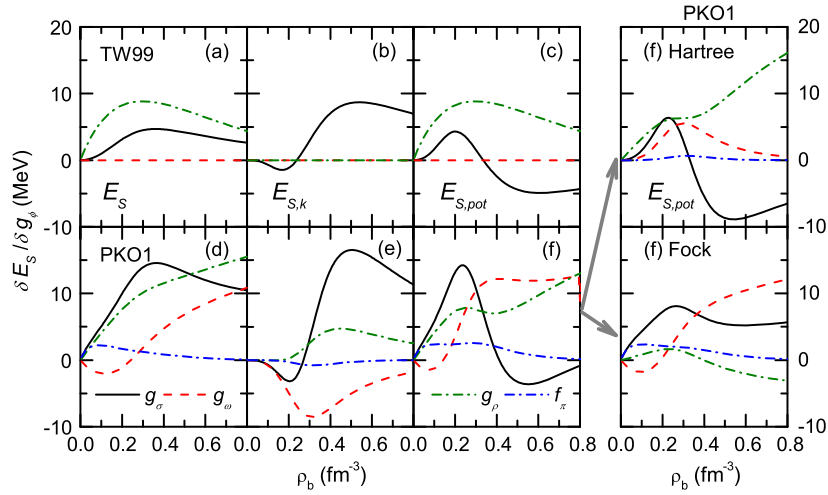


Figure 6. The first-order variation of total symmetry energy E_S (a), (d), kinetic symmetry energy $E_{S,k}$ (b), (e), and potential symmetry energy $E_{S,pot}$ (c), (f) with respect to various coupling constants g_σ , g_ω , g_ρ , and f_π . The results are calculated by the RMF model TW99 (a)–(c) and the RHF model PKO1 (d)–(f). The panel (f) is decomposed further into Hartree and Fock contributions in the right.

when they are extrapolated to the density region beyond ρ_0 . Thus, it is necessary to perform the error estimates of the predicted values in the above discussions, especially at supranuclear densities. Usually one should take the method of least-squares regression analysis to give the error estimates of theoretical models quantitatively [22–25], which is quite difficult to quantify. Since we focus on the role of the Fock terms in deciding the symmetry energy, a simplified method, i.e., doing a variation of E_S with respect to each of the meson-nucleon coupling constants, is used here to estimate the CDF model uncertainties of the symmetry energy.

It is seen in figure 6 that in the RMF, the theoretical model uncertainties of E_S arise only from g_ρ and g_σ , while in the RHF they are from all couplings due to the inclusion of the Fock terms. For the variation of the kinetic part $E_{S,k}$, a minus value is obtained around the saturation density by g_σ and g_ω , which could reduce the value of $E_{S,k}$ at ρ_0 dramatically. Besides, the model uncertainties of E_S in the RHF model become more evident than in the RMF at high densities. By separating the results into the contributions from the kinetic energy and the Hartree and Fock terms of the potential energy in the RHF, it is found that at high densities, g_σ variation plays the dominant role in the model uncertainties of $E_{S,k}$, while g_ρ and g_ω govern the model uncertainties in the Hartree and Fock terms of $E_{S,pot}$, respectively. A stringent constraint on the equation of state at supranuclear densities from terrestrial experiments or astrophysical observations could be helpful to improve the RHF EDF and reduce the uncertainties in predicting E_S .

4. Summary

In this paper, the density dependence of the nuclear symmetry energy E_S is studied in the CDF theory in terms of kinetic energy and the isospin-singlet ($T=0$) and isospin-triplet ($T=1$) potential energy parts of the EDF. We find that the $T=0$ potential contribution $E_{S,T=0}$

is strongly dominated by the Hartree terms in the σ - and ρ -meson coupling channels, while the $T = 1$ potential contribution $E_{S,T=1}$ is governed by the balance among various coupling channels. Especially at high densities, a rather significant contribution arises from the Fock terms of σ - and ω -mesons. It is shown that in the CDF calculations both the $T = 0$ and $T = 1$ potential components play an important role in determining the symmetry energy, especially in the RHF cases, thus demonstrating the importance of the Fock diagram (in particular from the isoscalar-meson coupling channels) in the isospin-related physics. It shows a different physical mechanism in determining the symmetry energy from the microscopic BHF case [45]. In addition, the inclusion of the Fock terms in the CDF theory changes the isospin dependence of the scalar self-energy and correspondingly leads to the reduced kinetic energy contribution to the symmetry energy, which could be regarded partly as the effects of the nuclear tensor-force components. Finally, the influence of the CDF model uncertainties on the symmetry energy is examined as well.

Acknowledgments

The authors are grateful to Or Hen and Bao-An Li for providing the data of the CFG model and assistance that led to improvements in the manuscript. The authors thank Xiao Jun Bao for his stimulating discussions. This work is partly supported by the National Natural Science Foundation of China (Grant Nos. 11205075 and 11375076) and the Specialized Research Fund for the Doctoral Program of Higher Education (Grant Nos. 20120211120002 and 20130211110005).

References

- [1] Brown B A 2000 *Phys. Rev. Lett.* **85** 5296
- [2] Horowitz C J and Piekarewicz J 2001 *Phys. Rev. Lett.* **86** 5647
- [3] Sun B Y, Long W H, Meng J and Lombardo U 2008 *Phys. Rev. C* **78** 065805
- [4] Long W H, Sun B Y, Hagino K and Sagawa H 2012 *Phys. Rev. C* **85** 025806
- [5] Centelles M, Roca-Maza X, Viñas X and Warda M 2009 *Phys. Rev. Lett.* **102** 122502
- [6] Tamii A *et al* 2011 *Phys. Rev. Lett.* **107** 062502
- [7] Li B A, Chen L W and Ko C M 2008 *Phys. Rep.* **464** 113
- [8] Newton W G, Murphy K, Hooker J and Li B A 2013 *Astrophys. J. Lett.* **779** L4
- [9] Quentin P and Flocard H 1987 *Annu. Rev. Nucl. Part. Sci.* **28** 523
- [10] Miller L D and Green A E S 1972 *Phys. Rev. C* **5** 241
- [11] Boguta J and Bodmer A 1977 *Nucl. Phys. A* **292** 413
- [12] Boguta J and Stocker H 1983 *Phys. Lett. B* **120** 289
- [13] Serot B D and Walecka J D 1986 *Adv. Nucl. Phys.* **16** 1
- [14] Chen L W, Ko C M and Li B A 2005 *Phys. Rev. C* **72** 064309
- [15] Chen L W, Ko C M and Li B A 2007 *Phys. Rev. C* **76** 054316
- [16] Akmal A, Pandharipande V R and Ravenhall D G 1998 *Phys. Rev. C* **58** 1804
- [17] Dalen V E, Fuchs C and Faessler A 2005 *Phys. Rev. C* **72** 065803
- [18] Li Z H and Schulze H J 2008 *Phys. Rev. C* **78** 028801
- [19] Taranto G, Baldo M and Burgio G F 2013 *Phys. Rev. C* **87** 045803
- [20] Lopes L L and Menezes D P 2014 *Phys. Rev. C* **89** 025805
- [21] Danielewicz P and Lee J 2014 *Nucl. Phys. A* **922** 1
- [22] Toivanen J, Dobaczewski J, Kortelainen M and Mizuyama K 2008 *Phys. Rev. C* **78** 034306
- [23] Reinhard P G and Nazarewicz W 2010 *Phys. Rev. C* **81** 051303
- [24] Kortelainen M, Lesinski T, Moré J, Nazarewicz W, Sarich J, Schunck N, Stoitsov M V and Wild S 2010 *Phys. Rev. C* **82** 024313
- [25] Dudek J, Szpak B, Porquet M G, Molière H, Rybak K and Fornal B 2010 *J. Phys. G: Nucl. Part. Phys.* **37** 064301

- [26] Dobaczewski J, Nazarewicz W and Reinhard P G 2014 *J. Phys. G* **41** 074001
- [27] Nikšić T, Paar N, Reinhard P G and Vretenar D 2015 *J. Phys. G* **42** 034008
- [28] Piekarewicz J, Chen W C and Fattoyev F J 2015 *J. Phys. G* **42** 034018
- [29] Roca-Maza X, Paar N and Colò G 2015 *J. Phys. G* **42** 034033
- [30] Long W H, Giai N V and Meng J 2006 *Phys. Lett. B* **640** 150
- [31] Long W H, Sagawa H, van Giai N and Meng J 2007 *Phys. Rev. C* **76** 034314
- [32] Long W H, Sagawa H, Meng J and van Giai N 2008 *EPL* **82** 12001
- [33] Long W H, Nakatsukasa T, Sagawa H, Meng J, Nakada H and Zhang Y 2009 *Phys. Lett. B* **680** 428
- [34] Long W H, Ring P, van Giai N and Meng J 2010 *Phys. Rev. C* **81** 024308
- [35] Long W H, Ring P, Meng J, van Giai N and Bertulani Carlos A 2010 *Phys. Rev. C* **81** 031302(R)
- [36] Lu X L, Sun B Y and Long W H 2013 *Phys. Rev. C* **87** 034311
- [37] Wang L J, Dong J M and Long W H 2013 *Phys. Rev. C* **87** 047301
- [38] Wang L J, Sun B Y, Dong J M and Long W H 2013 *Phys. Rev. C* **87** 054331
- [39] Jiang L J, Yang S, Sun B Y, Long W H and Gu H Q 2015 *Phys. Rev. C* **91** 034326
- [40] Liang H Z, van Giai N and Meng J 2008 *Phys. Rev. Lett.* **101** 122502
- [41] Liang H Z, Zhao P W and Meng J 2012 *Phys. Rev. C* **85** 064302
- [42] Liang H Z, Zhao P W, Ring P, Roca-Maza X and Meng J 2012 *Phys. Rev. C* **86** 021302(R)
- [43] Jiang L J, Yang S, Dong J M and Long W H 2015 *Phys. Rev. C* **91** 025802
- [44] Steiner A W, Prakash M, Lattimer J M and Ellis P J 2005 *Phys. Rep.* **411** 325
- [45] Vidaña I, Polls A and Providência C 2011 *Phys. Rev. C* **84** 062801(R)
- [46] Xu C, Li A and Li B A 2013 *J. Phys. Conf. Series* **420** 012090
- [47] Hu J N, Toki H and Ogawa Y 2013 *Prog. Theor. Exp. Phys.* **2013** 103D02
- [48] Carbone A, Polls A and Rios A 2012 *EPL* **97** 22001
- [49] Zhang X, Xu C and Ren Z Z 2014 *Eur. Phys. J. A* **50** 113
- [50] Hen O, Li B A, Guo W J, Weinstein L B and Piaseczky E 2015 *Phys. Rev. C* **91** 025803
- [51] Bouyssy A, Mathiot J F and van Giai N 1987 *Phys. Rev. C* **36** 380
- [52] Typel S and Wolter H H 1999 *Nucl. Phys. A* **656** 331
- [53] Long W H, Meng J, van Giai N and Zhou S G 2004 *Phys. Rev. C* **69** 034319
- [54] Ireland D G and Nazarewicz W 2015 *J. Phys. G* **42** 030301